Hexagonally ordered mesoporous ternary Li_2O–TiO_2–P_2O_5 oxides with high lithium content

Donglin Li,†[a] Haoshen Zhou,*[a] Itaru Honma[a] and Masaki Ichihara[b]

Received (in Cambridge, UK) 27th June 2005, Accepted 25th August 2005
First published as an Advance Article on the web 20th September 2005
DOI: 10.1039/b509028h

Hexagonally ordered mesoporous Li_2O–TiO_2–P_2O_5 oxides with high lithium content have been synthesized using surfactant-templated self-assembly; this ternary oxide has been specifically designed to yield a variety of mesoporous frameworks including a nanocomposite, amorphous multicomponent oxide, and almost fully nanocrystalline anatase.

Mesoporous oxides are of considerable interest in potential applications ranging from catalysis, sorption, chemical separation, to photonic and electronic devices. A great deal of effort has been devoted to developing mesoporous oxides since the 1990s. As a consequence, well-ordered mesoporous oxides of Si, Ti, Zr, W, Nb and Ta have been synthesized in the past several years[1–4]. A common feature for these materials is that the cations building up the oxides possess a high-valence oxidation state (tetravalent or higher) that easily form stable cation–oxygen tetrahedra or octahedra as building units to construct the oxide compound. However, a large number of multicomponent oxides in practical applications contain a high content of low-valence oxides (monovalent or bivalent). For example, alkali-metal oxides such as Li_2O are of considerable interest for composing ionically conductive materials and multicomponent compounds[5] for wide applications. To date, little work has been reported on high lithium-containing multicomponent mesoporous oxides, although these materials are highly desirable. In our previous studies on multicomponent mesoporous nanocomposites, we found that a small quantity of oxide M_xO_y (M = metal ion) ($\sim$5 mol%) can be doped in an ordered mesoporous TiO_2–P_2O_5 system,[6] indicating that it may be possible to synthesize multicomponent metal oxides containing low-valence metal ions. Herein, we describe a new result: the first recorded examples of mesoporous ternary Li_2O–TiO_2–P_2O_5 oxide with high lithium content, demonstrating that it may be possible, with the help of crystal chemistry theory, to synthesize mesoporous multicomponent oxides containing low-valence metal ions. Taking advantage of forming three-dimensional networks built from [TiO_6] octahedra or [PO_4] tetrahedra, in particular, of Li^+ locating in the amorphous network or structural channels of complex oxides, we found it possible to synthesize not only mesoporous, amorphous multicomponent oxides, but also a mesoporous framework of almost pure anatase by controlling the material composition.

In a typical synthesis,[6] 0.6–1.0 g of triblock copolymer HO-$(CH_2CH_2O)_{20}(CH_2CH(CH_3)O)_{70}(CH_2CH_2O)_{20}H$ ($(EO)_{20}(PO)_{70}$-$(EO)_{20}$, Pluronic 123, BASF) was dissolved in 6–8 g of ethanol. To this solution, 1.9 g of titanium tetraisopropoxide (Ti[OCH-$(CH_3)_2]_4$, TTIP) was added and the mixture was stirred for 10 min, forming a transparent solution in the presence of 0.3 g of 0.5 M HCl. Specifically, triethyl phosphate ($PO(OC_2H_5)_3$) and lithium chloride (LiCl) were added to this solution according to the designed composition x Li_2O–y TiO_2–z P_2O_5 (or LTP $x/y/z$; mole ratios). The multicomponent mixtures were stirred in a sealed bottle for 20 h. After transparent sols were gelled in an open Petri dish at room temperature in air for 5 days, the resulting transparent gels were dried at 80 °C for 7 days in an oven. The as-synthesized samples were calcined at 350 °C for 6 h to remove most of organic species, resulting in mesoporous, amorphous solids. Subsequently, the products were heat-treated at 400–500 °C for 1–2 h in air. The resulting materials were characterized by X-ray diffraction (XRD, MAS diffraction meter with Cu-Kα radiation), transmission microscopy (TEM, JEOL 1200EX), Barrett–Joyner–Halenda (BJH) analysis (Belsorp 18^+ A system), and an inductively coupled plasma analyzer (ICP, Therm Jarrell Ash IRIS/AP) for elemental analysis.

When the mesoporous, amorphous Li_2O–TiO_2–P_2O_5 oxides are heat-treated or sintered at 400–500 °C, the chemical structure of the materials will rearrange to lead to phase separation and crystallization through the mass transportation of atoms or ions, which may change the phase composition and microstructure of the materials on a nanometer or micrometer scale. Two-dimensionally (2-D) hexagonally mesoporous, amorphous Li_2O–TiO_2–P_2O_5 oxide can be produced over a wide composition range.

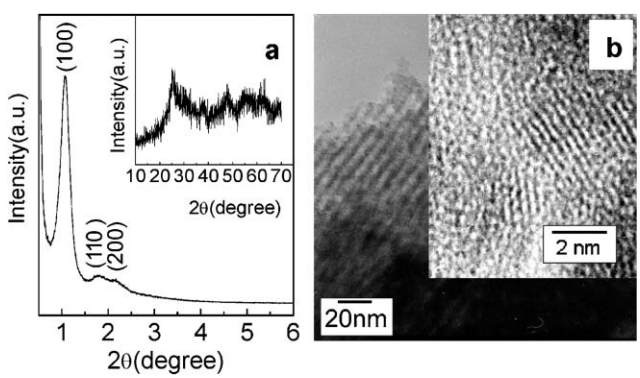

Fig. 1 SXRD and WXRD (inset) patterns (a) and TEM images (inset is HRTEM) (b) of the LTP58/66/66 material heat-treated at 400 °C.

[a]*Energy Electronics Institute, National Institute of Advanced Industrial Science and Technology (AIST), AIST Tsukuba Central, 1-1-1 Umezono, Tsukuba, Ibaraki, 305-8568, Japan. E-mail: hs.zhou@aist.go.jp*
[b]*Institute for Solid State Physics, University of Tokyo, Kashiwa, Chiba, 277-8581, Japan*
† Present address: Department of Applied Chemistry, Faculty of Engineering, University of Miyazaki, Gakuen Kibara-dai Nishi 1-1, Miyazaki, 889-2155 Japan. E-mail: donglinli@hotmail.com.

Because Li_2O makes the materials tend to crystallize during heat-treatment, while P_2O_5 prevents the materials to crystallize, the phase composition of the mesoporous framework changes with material composition. For the materials with both low Li_2O and P_2O_5 content (x, z = 2–5%), heat-treatment processing transformed the mesoporous, amorphous framework into a mesoporous nanocomposite consisting of both nano-sized anatase (3–6 nm) and multicomponent titanophosphate glass. This is similar to the results reported in our previous publication.[6] With increasing P_2O_5 content, the amorphous nature of mesoporous framework tends to increase. In the cases of high P_2O_5 content (z = 40% or higher), the mesoporous framework is usually amorphous after heat-treatment at 400–500 °C. Even if the content of Li_2O is high, the mesoporous framework is still amorphous before the ordered mesostructure collapses due to heat-treatment at higher temperature. Fig. 1 demonstrates a typically amorphous framework of the ordered mesopores in the high P_2O_5 content Li_2O–TiO_2–P_2O_5 oxide. The small-angle X-ray diffraction (SXRD) pattern of LTP 58/66/66 sample shows a 2-D hexagonal lattice with a lattice constant a = 95 Å in the space group *P6mm* (Fig. 1(a)). Transmission electron microscope (TEM) images revealed a clear arrangement of [110]-oriented cylindrical channels with uniform size (Fig. 1(b)). The mesoporous framework is macroscopically amorphous according to its wide-angle X-ray diffraction (WXRD) pattern (Fig. 1(a), inset), but tiny phase separation regions (1–2 nm) or nuclei were observed in TEM analyses (Fig. 1(b), inset). This type of ordered mesostructure remained stable at up to 450 °C.

To increase the degree of crystallization of the mesoporous framework, an important step forward has been to adjust the material composition. Ternary Li_2O–TiO_2–P_2O_5 systems containing a higher Li_2O content readily crystallize at relatively lower temperatures. In contrast, a high P_2O_5 content hinders crystallization. For example, LTP10/66/32 already crystallized at 400 °C, whereas the LTP10/66/70 system, with relatively higher P_2O_5 content, begins to crystallize at 500 °C. Therefore, the degree of crystallinity of the mesoporous framework can be controlled by rationally selecting the relative content of Li and P. When decreasing P_2O_5 content but increasing Li_2O content, a mesoporous framework with almost full anatase structure can be produced. In this case, the original mesoporous structure can be retained after the materials have almost fully crystallized even if an amorphous–crystalline transition occurs. The long-range mesoorder of the crystalline framework was confirmed by XRD scattering. 2-D hexagonal mesostructure was observed in the SXRD pattern, as shown in the powder XRD patterns of the LTP10/66/32 sample (Fig. 2(a)). The mean crystallite size of anatase calculated from the XRD pattern using the Scherrer

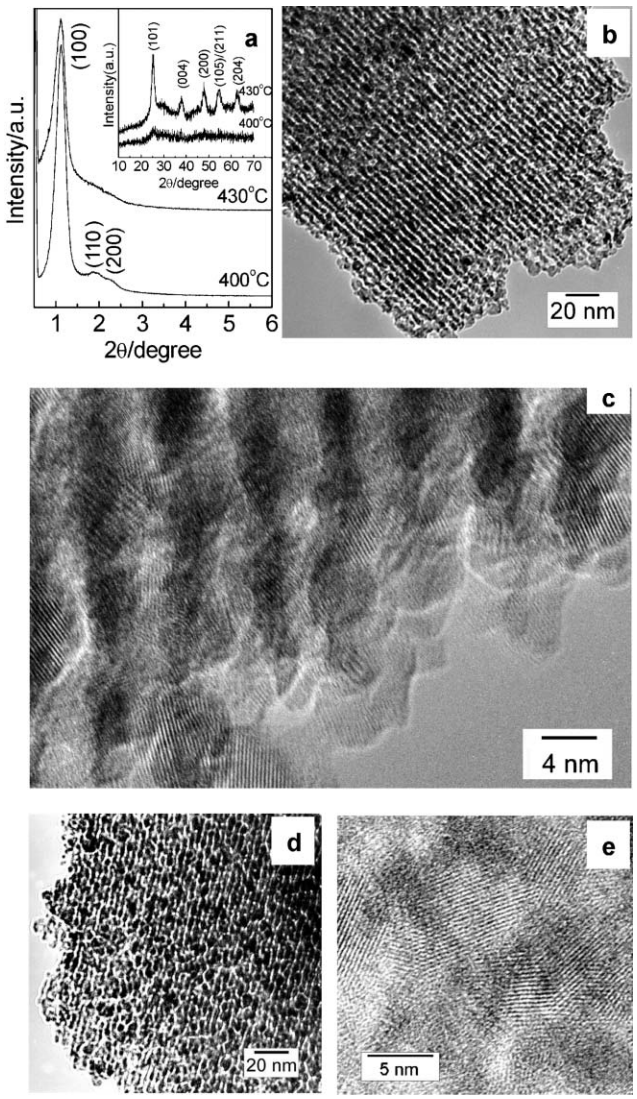

Fig. 2 Representative XRD patterns and TEM images of mesoporous Li_2O–TiO_2–P_2O_5 oxides with almost full anatase framework. (a) SXRD and WXRD (inset) patterns of LTP10/66/32 material. (b) Uniform [110]-oriented cylindrical channels in a mostly crystalline LTP10/66/32 sample derived upon heat-treatment at 430 °C. (c) Dense and overlapped lattice fringes of nanocrystals in parallel channels in the HRTEM image of crystalline LTP10/66/32 samples. The fringes wider than the crystal lattice fringes are Moiré fringes. (d) [110]-oriented channels in a mostly fully crystalline LTP22/66/32 sample derived upon heat-treatment at 400 °C, showing almost collapsed pore-wall structure. (e) Dense and overlapped lattice fringes of nanocrystals in the HRTEM image of (d).

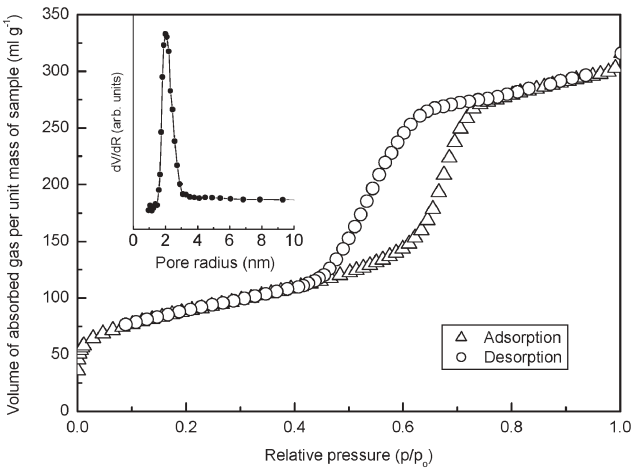

Fig. 3 Nitrogen adsorption–desorption isotherms and pore-size distribution plots (inset) from the desorption mode for LTP10/66/32 material heat-treated at 430 °C, showing clear capillary condensation and narrow distribution of pore size. The samples were degassed for 6 h at 150 °C before the analyses.

Table 1 Data of the structure and properties of hexagonally ordered mesoporous Li_2O–TiO_2–P_2O_5 oxides

Li/Ti/P (mole ratio)	Mesoporous framework	Crystal size/nm	T_s[a]/°C	T_c[b]/°C	Pore size/nm	BET/m^2 g^{-1}
2/66/32	Anatase + amorphous phase	4.2	450	500	4.3	287
5/66/32	Anatase + amorphous phase	4.7	430	450	3.9	225
10/66/32	Almost full anatase[c]	5.3	400	450	4.1	310
15/66/32	Almost full anatase	5.3	400	450	3.9	213
22/66/32	Almost full anatase	5.8	400	430	3.6	100
30/66/32	Almost full anatase	5.9	400	430	—	—
58/66/66	Amorphous	—	450	450	3.9	220
10/66/70	Amorphous	—	500	500	—	—

[a] T_s—Starting temperature of crystallization evaluated from XRD measurements. Threshold of T_c and T_s is 5 °C in the XRD measurements. [b] T_c—the collapse temperature of the most ordered mesophase evaluated from XRD measurements. [c] Almost full anatase means that the mesoporous framework is made up of nanocrystalline anatase and tiny quantities of amorphous phase.

equation was 5.3 nm for the sample annealed at 400 °C. TEM images provide direct evidence of the existence of the lattice fringes of nanocrystals in the ordered mesoporous framework, which overlap and freely stack along the walls of uniformly sized cylindrical channels (Fig. 2(b) and (c)). In the TEM analyses, Moiré fringes wider than the crystalline lattice fringes, which are resulting from the interference between the overlapped nanocrystalline lattices, was frequently observed, indicating high density of the nanosized anatase in the mesoporous framework. Elemental analysis from spatially resolved energy dispersive spectroscopy (EDS) in the TEM observation confirms the presence of titanium (Ti) and phosphorus (P). The presence of lithium (Li) was confirmed by inductively coupled plasma (ICP) analysis, since Li is too light to be analyzed in the TEM analyses. In addition, Li_2O was also indirectly identified by its influence on the crystallization of materials (see below).

Nitrogen adsorption–desorption isotherms confirmed the nature of uniform mesopores in the Li/Ti/P oxides, with a DH pore diameter of 3–5 nm and surface area of 200–300 m^2 g^{-1} using the BET (Brunauer–Emmett–Teller) method.[7] They are of Type IV with a gradual step at p/p_o = 0.5–0.8, indicating capillary condensation, which is typical of mesoporous solids (Fig. 3).

For a fixed P_2O_5 content, however, a higher Li_2O content tends to destroy the ordered mesopores during heat treatment. Here, we examine the effects of Li content on the mesostructure of the Li/Ti/P oxide at a molar ratio of *x*:66:32. With increasing Li content, the mesoporous framework changes from a nanocomposite consisting of anatase nanocrystals and Li_2O–TiO_2–P_2O_5 amorphous phase, to an almost full anatase (Fig. 2(b)–(e)), as described above in the LTP10/66/32 composition. Further increasing Li_2O content makes the mesoporous framework tend to became irregular or disordered. The TEM image in Fig. 2(d) demonstrates a typically irregular framework of mesopores in the LTP22/66/32 sample, indicative of the collapse of the ordered mesostructure (Fig. 2(d)). When increasing the Li_2O content up to x = 50, the ordered structure usually collapses during calcination for removing the organic agents (350 °C). Table 1 summarizes the structural data of materials with different lithium contents. For lower lithium content systems, the mesoporous, amorphous framework exhibits a relatively higher crystallization temperature. For example, mesoporous LTP22/66/32 material has already crystallized at 400 °C, whereas the LTP2/66/32 composition crystallizes above 450 °C. In contrast, the mesoporous materials containing higher P_2O_5 content retain amorphous solids. The mesoporous framework of the LTP58/66/66 sample remains amorphous even if heated up to 450 °C.

It should be pointed out that the ordered mesopores of the ternary Li_2O–TiO_2–P_2O_5 oxides collapsed if heated above 500 °C, irrespective of whether the materials were amorphous or crystalline. Obviously, the structural rearrangement of the materials during heat treatment, which can occur before the crystallization of materials, may destroy the ordered mesostructure in the ternary Li_2O–TiO_2–P_2O_5 system. It appears that the thermal stability of the mesostructure is closely associated with the crystal chemistry of oxides.

Donglin Li acknowledges the financial support of the Japanese Society of the Promotion of Science (JSPS) Fellowship for work carried out at Institute of Energy Electronics, National Institute of Advanced Industrial Science and Technology (AIST), Tsukuba Center, Japan. The authors are grateful for the partial research fund from JSPS, Japan.

Notes and references

1 (*a*) C. T. Kresge, M. E. Leonowicz, W. J. Roth, J. C. Vartuli and J. S. Beck, *Nature*, 1992, **359**, 710; (*b*) G. S. Attard, J. C. Glyde and C. G. Goltner, *Nature*, 1995, **378**, 366; (*c*) M. Templin, A. Franck, A. Du Chesne, H. Leist, Y. Zhang, R. Ulrich, V. Schadler and U. Wiesner, *Science*, 1997, **278**, 1795; (*d*) M. Trau, N. Yao, E. Kim, Y. Xia, G. M. Whitesides and I. A. Aksay, *Nature*, 1997, **390**, 674; (*e*) R. A. Pai, R. Humayun, M. T. Schulberg, A. Senupta, J.-N. Sun and J. J. Watkins, *Science*, 2004, **303**, 507.
2 A. Bhaumik and S. Inagaki, *J. Am. Chem. Soc.*, 2001, **123**, 691.
3 (*a*) N. K. Mal, S. Ichikawa and M. Fujiwara, *Chem. Commun.*, 2002, 112; (*b*) P. Yang, D. Zhao, D. I. Margolese, B. F. Chmelka and G. D. Stucky, *Nature*, 1998, **396**, 152; (*c*) Y. K. Hwang, K.-C. Lee and Y.-U. Kwon, *Chem. Commun.*, 2001, 1738; (*d*) B. Lee, D. Lu, J. N. Kondo and K. Domen, *J. Am. Chem. Soc.*, 2002, **124**, 11256.
4 T. Katou, B. Lee, D. Lu, J. N. Kondo, M. Hara and K. Domen, *Angew. Chem., Int. Ed.*, 2003, **42**, 2382.
5 (*a*) S. Wang and S.-J. Hwu, *J. Solid State Chem.*, 1991, **90**, 377; (*b*) M. Morales, L. Mestres, M. Dlouha, S. Vratislav and M.-L. Martinez-Sarrion, *J. Mater. Chem.*, 1998, **8**, 2691; (*c*) L. Bih, M. El Omari, J.-M. Reau, M. Haddad, D. Boudlich, A. Yacoubi and A. Nadiri, *Solid State Ionics*, 2000, **132**, 71; (*d*) L. Sebastian and J. Gopalakrisshnan, *J. Mater. Chem.*, 2003, **13**, 433; (*e*) P. D. Battle, C. P. Grey, M. Hervieu, C. Martin, C. A. Moore and Y. Paik, *J. Solid State Chem.*, 2003, **175**, 20.
6 D. Li, H. Zhou and I. Honma, *Nat. Mater.*, 2004, **3**, 65.
7 M. Kruk and M. Jaroniec, *Chem. Mater.*, 2001, **13**, 3169.